IEEE Access
Multidisciplinary | Rapid Review | Open Access Journal

Received March 12, 2021, accepted March 29, 2021, date of publication April 5, 2021, date of current version April 13, 2021.

Digital Object Identifier 10.1109/ACCESS.2021.3070837

Improved Smartphone-Based Indoor Localization System Using Lightweight Fingerprinting and Inertial Sensors

SANTOSH SUBEDI, DAE-HO KIM, BEOM-HUN KIM, AND JAE-YOUNG PYUN
Department of Information and Communication Engineering, Chosun University, Gwangju 501-759, South Korea

Corresponding author: Jae-Young Pyun (jypyun@chosun.ac.kr)

This work was supported by the National Research Foundation of Korea (NRF) Grant funded by the Korean Government (MSIT) under Grant NRF-2019R1A2C1004847.

ABSTRACT The existing radio frequency-based positioning approaches widely used for indoor localization-based service (LBS) are fingerprinting and trilateration and their integration with the inertial sensors-based dead reckoning system. However, these localization methods have practical limits and challenges due to unstable signal strength, the cost of offline workload, computational complexity, terminal device heterogeneity, and accumulated sensor error. We propose a smartphone-based indoor localization system using weighted Spearman's foot-rule (WSF)-based probabilistic fingerprinting for reliable smartphone localization service. This localization system adopts a real-time fingerprinting position error estimation approach realizing an adaptive extended Kalman filter (AEKF) to integrate the proposed fingerprinting localization with inertial measurement unit (IMU)-based localization. This proposed WSF-based smartphone localization uses a Gaussian process regression (GPR)-based signal prediction module to deal with fingerprinting localization's offline workload. Furthermore, the smartphone localization system's expected high computational complexity is controlled by employing a data-clustering module. The proposed WSF also employs a rank vector that helps mitigate the effect of terminal device heterogeneity. The proposed localization system is experimentally evaluated at two different representative indoor environments. Experimental results obtained by real field deployment show that the mean error is 2.06 m in an elongated hallway corridor and 3.47 m in the crowded and well-furnished wide area.

INDEX TERMS Adaptive EKF, Bluetooth low energy (BLE), data clustering, fingerprinting localization, inertial sensors, spearman's foot-rule, received signal strength (RSS).

I. INTRODUCTION

Over the years, the global navigation satellite system (GNSS) has been widely used for location-based services (LBS). However, the performance of GNSS in the indoor environment is poor; thus, many researchers around the world have actively explored a ubiquitous solution to indoor localization problems over the past decades.

Recent trends in addressing indoor localization problems are focused on using low-cost/cost-free infrastructure, data fusion, and machine learning and crowdsourcing approaches [1]–[5]. Radiofrequency (RF)-based wireless technologies are overwhelmingly used to realize indoor LBS (a.k.a indoor positioning system (IPS)) owing to properties like signal penetration, low power consumption, and good localization accuracy. For instance, Wi-Fi access points (AP) deployed in modern buildings are utilized as a signal source, and Bluetooth low energy (BLE) beacons are deployed as a low-cost solution. Besides RF-based technologies, magnetic fields [6], inertial measurement unit (IMU) sensors of smartphones [7], and visible light [8] are some alternative technologies.

The majority of the state-of-art positioning approaches use received signal strength (RSS) as a signal measurement metric. The RSS value can be obtained without extra hardware (using off-the-shelf smartphones), and an RSS-based positioning approach does not require any time synchronization among the transmitter-receiver pairs. However, the RSS in indoor spaces is attenuated and fluctuates randomly over time and space due to transmitter/receiver antennas, the material

The associate editor coordinating the review of this manuscript and approving it for publication was Kegen Yu.

of walls/floors, and people's movement and presence of obstacles [5]. Other metrics used for positioning in IPS are the time of arrival (TOA), time difference of arrival (TDOA), angle of arrival (AOA), and round-trip time. These metrics require either extra hardware or time synchronization for data reception.

Fingerprinting and trilateration are the widely used positioning techniques in IPS. Fingerprinting has a scene analysis process that consists of offline and online phases. The RF signature map (a.k.a fingerprinting map) is first built in the offline phase. The online phase deals with the localization estimation, where real-time RSS is compared with the RF signature map to deduce the user's position. Fingerprinting localization has been a prime choice for researchers owing to its good localization accuracy and non-requirement of line-of-sight measurements of APs. However, data acquisition in the offline phase is time-consuming, and labor-intensive [9]. Similarly, trilateration estimates the location of the user by estimating his/her distance from multiple APs. Here, both TDOA and RSS can be utilized to deduce the distance from the AP.

However, an IPS designed to localize a smartphone using an RF-based wireless technology faces challenges like complex indoor environment, RSS fluctuation, terminal device heterogeneity, costly data learning methodology for scene analysis, computational complexity, and system cost. These issues escalate practical limits and challenges to develop a reliable and scalable IPS. Hence, an efficient and reliable IPS should possess acceptable localization accuracy, scalable/robust system, minimum computational complexity, and feasible system cost. Meanwhile, current indoor localization solutions are employed to acquire the discussed IPS characteristics. For example, the IPS presented in [10] combines several technologies to achieve good localization accuracy; however, it is less robust/scalable and has great computational complexity. Similarly, a Gaussian process assisted fingerprinting approach is proposed in [4], where the RF signature map is predicted using a regression process trained by a few RF signature datasets. This approach reduces the cost of offline workload; however, it still has several meters of localization estimation error.

This paper presents a simple yet effective localization system for integrating multisensory data by using an extended Kalman filter (EKF) [11], [12]. In particular, the suggested IPS yields better localization estimation while reducing both the offline workload and online computational complexity.

An overview of the proposed localization system is shown in Fig.1. For this localization system, we propose (a) a weighted Spearman's foot-rule (WSF)-based probabilistic fingerprinting localization, (b) a real-time fingerprinting position error ($\hat{\epsilon}$) estimation approach to determine the dynamic measurement noise, and (c) an adaptive EKF (AEKF) employing $\hat{\epsilon}$ to adaptively integrate data from IMU sensors and BLE beacon. To reduce the cost of offline data collection, we model the BLE beacons' signal as a Gaussian process (GP) and implement GP regression (GPR)

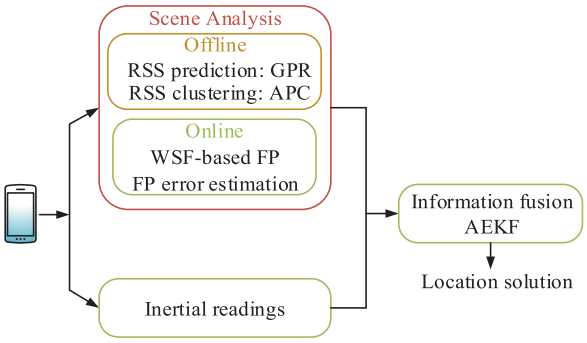

FIGURE 1. The framework of the proposed localization system. (FP: fingerprinting position).

to predict the RSS over the area of interest for localization. In addition, data clustering is shown to reduce the computational complexity of the system.

This paper is organized as follows. In Section II, a review of pertinent literature is presented, and motivation and problem formulation are described in Section III. Section IV introduces a general model of Spearman's foot-rule (SF), GPR, and affinity propagation clustering (APC). Section V elaborates on the system design of the proposed localization system. The experimental results and discussion are presented in Section VI. Finally, the conclusions are drawn in Section VII.

II. RELATED WORKS

A. MULTISENSORY DATA INTEGRATION

Although various systems and solutions for IPS are presented in different state-of-art approaches, there is no fixed set of rules that serve as a guide for designing an IPS [13]. Hence, an optimal localization strategy is still an open issue. At present, integrating the low-cost IMU-based pedestrian dead reckoning (PDR) system with the RF-based positioning systems has been a trending localization solution. In particular, EKF is utilized for data fusion, where the measurement model and state model are developed with fingerprinting estimation and the PDR system, respectively [7], [11], [12].

The enhanced localization solution presented in [7] integrates IMU, wireless, and magnetic sensors using EKF for mass-market location-based IoT applications. This work proposes using a fingerprinting accuracy indicator as a diagonal element of the measurement noise matrix, making the measurement noise inconstant and stopping the degradation of the sensors' integration solution. The next example of sensor fusion is presented in [11], where wireless and IMU sensors are fused with two different EKFs. The first EKF is utilized to combine the gyroscope and accelerometer data for the heading estimation of PDR. Later, the second EKF yields the location estimation by integrating Wi-Fi fingerprinting and the PDR system. Here, spatial filtering that uses earlier localization estimation to narrow-down the RP search space is proposed. A similar method was proposed in [12], wherein threshold distance-based weightage was assigned to Wi-Fi and PDR positioning methods during EKF integration.

B. RSS PREDICTION

A machine-learning algorithm extracts useful information from a raw data set and represents it as a model or hypothesis applied to other data to make inferences. Hence, machine learning algorithms (for instance, GPR and support vector machine (SVM)) can be utilized in IPS to predict the RSS data at non-site-surveyed locations on the testbed. RSS data prediction across the testbed with little training data significantly reduces the human workload in the offline phase of fingerprinting localization.

The GPR has gained much attention in the machine learning community in recent decades [14]. It can be defined as a supervised learning task that can predict the RSS at arbitrary coordinates based on acquired training RSS data. GPR-based fingerprinting localization is presented in [4], wherein reduced Wi-Fi RSS data were used to train the GP and the firefly algorithm to estimate the hyperparameters of the GP. This study also shows that the probabilistic fingerprinting method yields better localization accuracy compared to the deterministic one. Furthermore, a GPR-plus method using Bluetooth transmitters is proposed in [15], where the Naïve Bayes algorithm is used for localization. This study's results are compared with those of [4] to show that their method is computationally cheaper. Another example of GPR-based fingerprinting is presented in [16], where BLE beacons are utilized for localization. Here, the hyperparameters of GP are optimized using the limited-memory Broyden—Fletcher—Goldfarb—Shanno (LM-BFGS) algorithm [17], [18].

Furthermore, Kumar *et al.* adopt a subspace trust-region method in [19] to optimize the hyperparameters of the GP and claim that their approach yields better localization results compared to HORUS [20]. Note that the discussed GPR-based methods choose ''random'' places for training data measurement and no specific set of rules are provided.

Like GPR, the SVM has also been utilized to estimate the RSS of APs at non-site-surveyed locations. For example, [21] uses SVM to estimate the Wi-Fi signal strength across the testbed. They created an RSS reference surface for each AP utilizing the discrete train data with SVM. During the online phase, the online RSS freshly acquired from each AP is searched in the corresponding surfaces. The coordinate found in the higher number of such surfaces is used to estimate the device location.

C. DATA CLUSTERING

Traditional flat fingerprinting localization requires searching at every RP to find the best-fingerprinting match. Flat fingerprinting is improvised into two-step fingerprinting using data clustering, which reduces the search space of RPs. It will induce a better localization result with a low computational cost. Clustering on IPS can be realized in two different ways: device and RSS clustering, as shown in Fig. 2.

In terms of device-based clustering, the earliest work using a clustering module based on a hardware device is the HORUS [20]. Here, a cluster is defined as a set of RPs

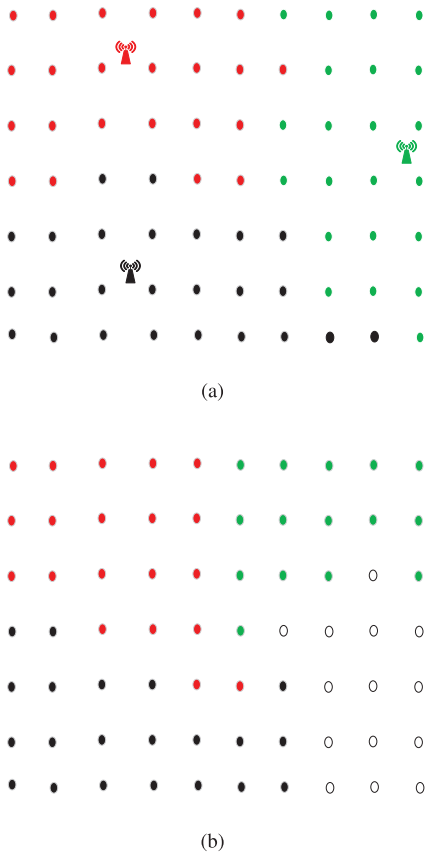

FIGURE 2. Illustration of clustering in IPS where each dot represents an RP: (a) device-based (proximity) clustering and (b) RSS clustering.

sharing a common set of Wi-Fi APs. This method estimates the tag position based on the largest posterior probability by Bayesian inference. Similarly, [22] proposes a BLE beacon proximity-based clustering module. Here, coarse localization is performed with the BLE beacon's proximity, and fine localization is followed by using a selected set of RPs with Wi-Fi fingerprint data sets.

An RSS clustering method chooses a set of cluster centers by measuring the sum of squared distances between the RSS data and their corresponding centers. For instance, a K-means clustering begins by choosing both the size of the output clusters and their initial cluster heads, where output clusters are iteratively refined by finding the sum of the squared distances [23]. Another RSS clustering method widely employed in IPS is APC, which starts by assigning each point (RP in this paper) the same chance to become a cluster center where all the RPs are joined in the large space [24]. In addition to K-means and APC, some representative clustering approaches in IPS include fuzzy c-means, and the hierarchical clustering strategy [25]. Numerous studies on IPS have employed APC for RSS clustering owing to its initialization independence and better cluster head selection characteristics [12], [26], [27].

III. MOTIVATION AND PROBLEM FORMULATION

As the area of interest for fingerprinting localization grows, offline workload increases [16]. Moreover, the RF signature

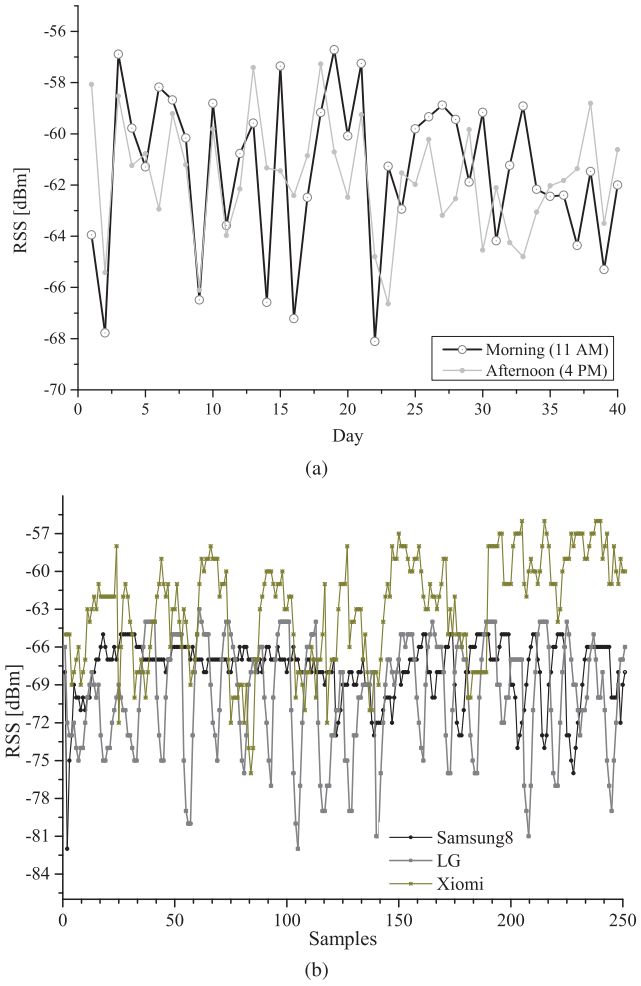

FIGURE 3. (a) RSS observed at an identical indoor location at different times, and (b) RSS samples acquired by multiple terminal devices at an identical indoor location.

map needs to be updated from time to time to attain good localization estimation owing to the dynamic and unpredictable nature of the radio channel, and changes in the testbed environment [4]. For instance, we collected the RSS data from an average of 35 BLE RSS samples at a single epoch at a fixed measurement place for 40 d (two times a day) as presented in Fig. 3a.

In Fig. 3a, the RSS data are not shown as stable, which suggests a frequent radio database update. Because constructing a single set of RF signature map is work-intensive, performing frequent map updates is considerably tedious.

Furthermore, the calibrated data (RF signature, path loss exponent, etc.) in various tag devices can be different owing to the dissimilar gains of receivers and antennas [2]. To observe the effect of terminal device heterogeneity, we acquired RSS data from a BLE beacon by using different Android devices (Samsung Galaxy S8, LG G7, and Xiaomi MI Redmi 4). The observed result is shown in Fig. 3b.

The existing issues of typical RF-based IPS and the observed data motivated us to design a positioning method with lightweight workload features, low computation, flexibility, and stable localization results for use in heterogeneous terminal devices.

We consider a 2-D area $\Lambda \triangleq \mathbb{R}^2$ covered by U BLE beacons, which is divided into non-overlapping hypothetical RPs given as

$$\varphi_i \triangleq (x_i, y_i) \in \Lambda. \tag{1}$$

The RSS from beacon $u, (1 \leq u \leq U)$ at location φ_i is denoted as $f_u(\varphi_i)$, which fluctuates over time owing to a complex indoor environment. The offline phase of conventional fingerprinting consists of RSS data measurement at each RP given as follows:

$$\omega_u(\varphi_i) = f_u(\varphi_i) + \vartheta. \tag{2}$$

Here, ϑ is an independent and identically distributed Gaussian noise with zero mean and variance (σ_ϑ^2) summarized as $\vartheta \sim N(0, \sigma_\vartheta^2)$. Hence, the RF signature map consists of the RSS received from each beacon at each RP. The constructed RF signature map can be utilized for online localization. As the RF signature map construction in conventional fingerprinting localization is burdensome, one of our goals is to minimize the offline workload by only taking the RF signature data at a subset of the locations training the GP to predict the RF signature map.

Let the predicted RF signature map be represented as

$$\Psi = \begin{pmatrix} \psi_{1,1} & \psi_{1,2} & \cdots & \psi_{1,N} \\ \psi_{2,1} & \psi_{2,2} & \cdots & \psi_{2,N} \\ \vdots & \vdots & \ddots & \vdots \\ \psi_{U,1} & \psi_{U,2} & \cdots & \psi_{U,N} \end{pmatrix}, \tag{3}$$

where N is the total number of RPs in the localization area. As we aim to reduce computational complexity, we preprocess the predicted data for data clustering. Moreover, the RF fingerprint at j^{th} RP, $\Psi_j = \{(\psi_{1,j}, \psi_{2,j}, \ldots, \psi_{U,j})^T | j = 1, \ldots, N\}$ is rearranged in descending order to form a rank vector R_j. The rank vector will be a solution dealing with the terminal device heterogeneity problem.

In the online phase, the tag device measures the RSS of the surrounding beacons at an unknown location (r'), $\Psi'_{r'} = (\psi_{1,r'}, \psi_{2,r'}, \ldots, \psi_{U,r'})$. As the received online RSS is attenuated by noise; a noise filter is applied to acquire a smooth estimation, $\widehat{\Psi'_{r'}} = F(\Psi'_{r'})$.

The objective of a fingerprinting localization scheme is to estimate the tag location, $\hat{L} = (\hat{x}, \hat{y})$, based on a guideline (G) that finds the closest match by comparing the online RSS against the RF signature map as

$$\hat{L} = G(\Psi, \widehat{\Psi'_{r'}}). \tag{4}$$

Also, to further deal with the interference and instability phenomena of RSS (that can result in inconsistent localization estimation even at a fixed place), we employ a real-time fusion scheme using AEKF combining fingerprinting and PDR localization:

$$\hat{E} = AEKF(\hat{L}, PDR), \tag{5}$$

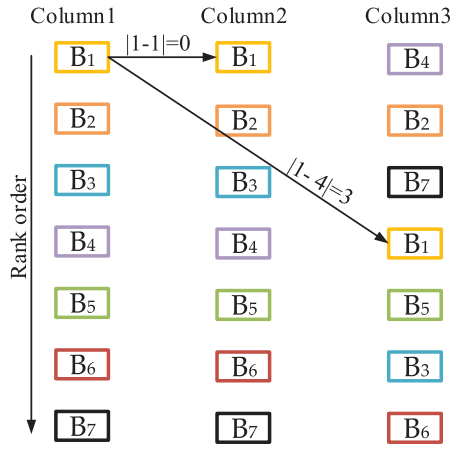

FIGURE 4. Illustration of the SF distance computation where $(B_1, B_2, \ldots.., B_7)$ represent BLE beacons.

where $\hat{E}$ is the localization estimation of the proposed method. Here, the dynamic noise of the filtering system is adaptively determined.

IV. ADOPTED TECHNOLOGIES FOR THE PROPOSED INDOOR LOCALIZATION SYSTEM

A. SPEARMAN'S FOOT-RULE

Spearman's measure of disarray is the sum of the absolute values of the differences between the ranks [28]. In other words, Spearman's foot-rule (SF) distance measures total elementwise displacement between two permutations or ranked lists [29]. The SF distance can be used in several statistical problems in different fields that require the assessment of agreement or disagreement between two sets of measurements.

To derive the SF distance, let us consider $[n] = \{1, 2, \ldots, n\}$ as a collection of elements. Furthermore, let P_n be the set of permutations on $[n]$ where $\Theta \in P_n$ and $\Theta(i)$ denotes the rank of element i. Here, the SF distance between two permutations, $\Theta, \alpha \in P_n$ is denoted as $SF(\Theta, \alpha)$. Meanwhile, [29] states that the SF distance does not depend on the actual identity of elements and considers $SF(\Theta) = SF(\Theta, 1)$, where 1 is the identity permutation. Hence, the formal definition of SF distance is given as

$$SF(\Theta) = \sum_i |i - \Theta(i)|. \tag{6}$$

In our implementation, considering $R_j|j = 1, 2, \ldots, N$, as a rank vector, we generalized the SF distance to incorporate element distance as follows:

$$SF(j) = \sum_{i=1}^{U} |R_j(i) - R_{online}(i)|, \tag{7}$$

where $R_j(i)$ represents the rank order of the i^{th} beacon at the j^{th} RP from the RF fingerprint map and $R_{online}(i)$ is the rank order of the i^{th} beacon at the online phase. For instance, let us consider the three columns of Fig. 4, where *column*1 is compared to *column*2 and *column*3 for similarity comparison. As the SF distance of *column*1 is less with *column*2 compared to *column*3, *column*1 and *column*2 have good agreement. Furthermore, we propose assigning a certain weight to the SF distance of each RP to form a WSF owing to the instability of the RSS in an indoor environment.

B. GPR FOR FINGERPRINTING LOCALIZATION

A GP is a collection of random variables $f(\boldsymbol{\varphi}|\boldsymbol{\varphi} \in \chi)$ (χ is the index set of possible input values) where any finite subset of realizations of the process $f = \{f(\boldsymbol{\varphi})\}_{i=1}^{m}$ is jointly Gaussian distributed [30]. It is also a generalization of a normal multivariate distribution in a finite dimension where it defines a distribution over functions from the view of function space [4], [30]. The GP is fully specified by its mean function $m(\boldsymbol{\varphi}) = \mathbb{E}[f(\boldsymbol{\varphi})]$ and covariance function $k(\boldsymbol{\varphi}_q, \boldsymbol{\varphi}_r) = \mathbb{E}[(f(\boldsymbol{\varphi}_q) - m(\boldsymbol{\varphi}_q))(f(\boldsymbol{\varphi}_r) - m(\boldsymbol{\varphi}_r))]$, where $\mathbb{E}[.]$ is the expectation operator [5].

Rewriting (2), we get

$$A = f(b) + \vartheta, \tag{8}$$

where A denotes the RF signature observation, and b is the 2-D location coordinate (input features) of RPs. From (8), it can be inferred that the regression problem consists of constraining the non-linear function $f(.)$ from the noisy observations that arise from σ_ϑ^2. The inference of $f(b)$ corresponds to estimating the posterior distribution as

$$p(f(b)|A, B) = \frac{p(A|f(b), B)p(f(b))}{p(A|B)}, \tag{9}$$

where $p(A|f(b), B)$ represents the probability (likelihood function) of acquiring A given $f(b)$, where B is the $2 \times N$ matrix of input features.

In the context of RF signatures, the GPR employs the covariance of neighboring RSS to predict the RSS at arbitrary locations where the covariance is based on kernel functions. Note that the kernel function decreases with the increased distance of the input points and peaks when the input space distance is minimal. Typical kernel functions employed in RF signature prediction are Gaussian, Laplacian, and exponential. It was reported in [19] that the localization accuracy is relatively insensitive to the kernel function's choice. In this study, we have employed the widely adopted squared exponential kernel function:

$$k(b_q, b_r) = \sigma_f^2 \exp^{-} \frac{(\|b_q - b_r\|)}{2l^2}, \tag{10}$$

where σ_f^2 is the signal variance, l is the length scale parameter that characterizes the smoothness of a function, and $\|.\|$ is the L_2 norm representing the Euclidean distance between two vectors. Assuming the covariance matrix of all pairs of training targets as $K(B, B)$, the covariance function of the prior distribution becomes

$$cov(A) = K(B, B) + \sigma_\vartheta^2 I, \tag{11}$$

where I is an identity matrix.

Now, $f(b)$ in terms of the Gaussian process can be stated as

$$f(b) \sim \mathcal{GP}\Big(m(b), k(b_q, b_r)\Big). \tag{12}$$

As GP modeling assumes that the data (training A and predicted A^* beacon data) can be represented as a sample from a multivariate Gaussian distribution, the joint Gaussian distribution of target values assuming the zero-mean prior distribution is given as

$$\begin{bmatrix} A \\ A^* \end{bmatrix} \sim N\Big(0, \begin{bmatrix} K(B,B) + \sigma_\vartheta^2 I & K(B,B^*) \\ K(B^*,B) & K(B^*,B^*) \end{bmatrix}\Big), \tag{13}$$

where $K(B, B^*)$ is a $N \times N^*$ matrix containing the covariance between all pairs of A and A^*. The conditional probability of $A^*|A$ is computed as

$$P(A^*|A) \sim N\Big(K(B^*,B)[K(B,B) + \sigma_\vartheta^2 I]^{-1}A), K(B^*,B^*) - K(B^*,B)[K(B,B) + \sigma_\vartheta^2 I]^{-1}K(B,B^*)\Big). \tag{14}$$

Here, $P(A^*|A)$ indicates how likely a prediction A^* is, given the training data A. From (14), the mean function and covariance function can be inferred as

$$\mu_* = K(B^*,B)[K(B,B) + \sigma_\vartheta^2 I]^{-1}A). \tag{15}$$

$$\sigma_*^2 = K(B^*,B^*) - K(B^*,B)[K(B,B) + \sigma_\vartheta^2 I]^{-1}K(B,B^*). \tag{16}$$

Hence, the GPR can be utilized to build an RF signature map with a predicted mean (15) and variance (16) for locations without prior measurements. The resulting map can then be employed for online localization estimation.

The principal structure of the GP model is determined by the mean and covariance functions; however, to fit the observations properly, the function's optimal hyperparameters, $\theta = [\sigma_f, l]$ in (10) need to be established. There are various ways of inferring the GP hyperparameters, such as marginal likelihood, Bayesian optimization, and cross-validation [30]–[32]. The marginal likelihood is optimal and computationally efficient when the data truly follow the GP model. The marginal likelihood is also implemented with tools such as the maximum a posteriori estimator and minimum mean square error estimator. The logarithmic form of the marginal likelihood function for Gaussian distributed noise is

$$\log\{p(A|B,\theta)\} = -\frac{1}{2}A^T[K(B,B) + \sigma_\vartheta^2 I]^{-1}A - \frac{1}{2}\log|K(B,B) + \sigma_\vartheta^2 I| - \frac{\vartheta}{2}\log 2\pi, \tag{17}$$

where T denotes the matrix transpose.

C. APC FOR RSS DATA CLUSTERING

The APC joins all of the points in the large space and makes each point node (RP in our case) a potential exemplar. The points launch a responsibility message and receive an availability message constantly that continues to extend the gap between the exemplar and supplementary points until the exemplar is decided [24], [26]. Let ψ_i and ψ_j denote the mean RSS vectors of any two RPs, the similarity between the RPs indicated by $s(i, j)$ is written as:

$$sim(i,j) = -\|\psi_i - \psi_j\|^2, \forall i,j \in \{1,2,\ldots,N\}. \tag{18}$$

The similarity values form a $N \times N$ similarity matrix Z, where N is the total number of RPs to be clustered. The value $(sim(j, j))$ on the diagonal of the matrix Z is called self-similarity, is used to judge whether RP_i can become the exemplar. The self-similarity is also known as a preference $(Pref)$ as:

$$Pref = median\{sim(\psi_i - \psi_j), i \neq j, \forall i,j \in \{1,2,..,N\}\}. \tag{19}$$

The responsibility and availability messages transmitted by RPs are denoted as $r(i, j)$ and $a(i, j)$, respectively. Note that both of them are set to zero initially. The responsibility message represents the confidence level of RP_j as an exemplar of RP_i, which is updated as:

$$r(i,j) = sim(i,j) - \max_{j' \neq j}\Big\{a(i,j') + sim(i,j')\Big\}. \tag{20}$$

The availability message represents that RP_i selects RP_j as the confidence center of its exemplar, which is updated as:

$$a(i,j) = min\Big\{0, r(j,j) + \sum_{i' \neq i,j} max\{0, r(i',j')\}\Big\}. \tag{21}$$

Moreover, $a(j, j)$ is a self-availability message that represents the cumulative evidence for RP_i as the exemplar calculated as:

$$a(j,j) = \sum_{i' \neq j} max\{0, r(i',j)\}. \tag{22}$$

In order to avoid the possible ringing oscillation while updating (20) and (21), a damping factor (γ) $[0.5, 1)$ is exploited resulting in the following equations

$$r_t = \gamma \times r_{t-1} + (1-\gamma) \times r_t$$
$$a_t = \gamma \times +(1-\gamma) \times a_t. \tag{23}$$

Here, r_t and a_t corresponds to the value of responsibility and availability of the current iteration, respectively. Similarly, r_{t-1} and a_{t-1} are the value of responsibility and availability of the last iterations. The exemplar is updated according to the value of $r(i, j) + a(i, j)$. If $r(i, j) + a(i, j)$ is largest, it denotes that RP_j is the exemplar of RP_i. Else, RP_i will be selected.

V. DESIGN OF THE PROPOSED INDOOR LOCALIZATION SYSTEM

Figure 5 shows the system diagram for the proposed localization method. The components of the system architecture presented in Fig. 5 are explained in the upcoming sections.

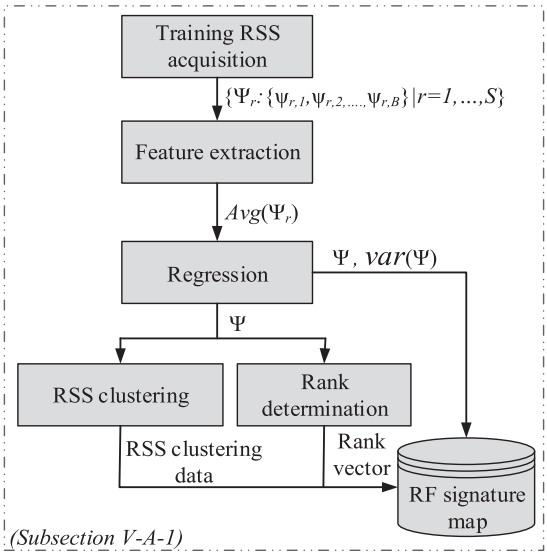

(a)

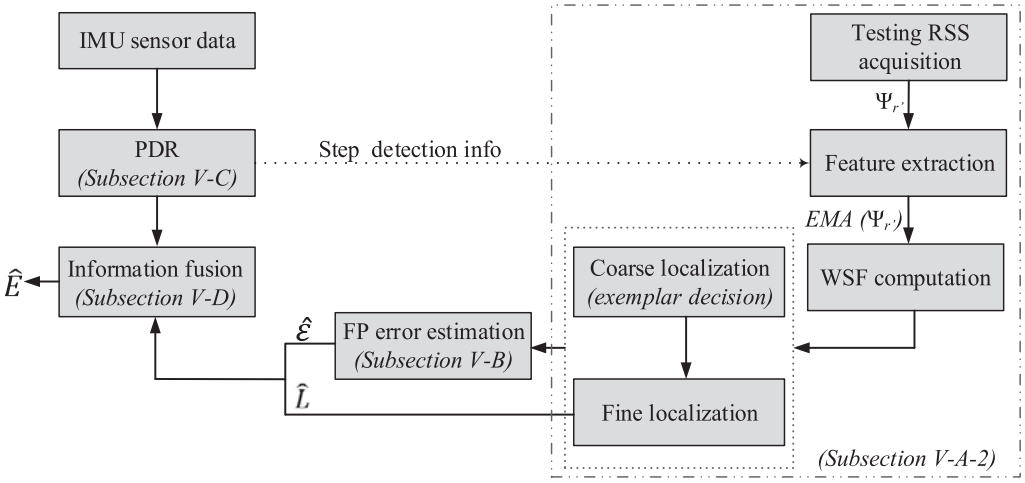

(b)

FIGURE 5. Proposed indoor localization model: (a) RF signature map creation and (b) location estimation.

A. WSF-BASED PROBABILISTIC FINGERPRINTING LOCALIZATION

Typical fingerprinting localization compares the newly acquired RSS and the stored RF signature map to estimate a current location. The metrics employed for signal comparison classify the existing fingerprinting localization into deterministic and probabilistic localization. The former method searches for the closest signal strength match depending on signal distance, whereas the latter approach obtains location information by estimating a probability distribution over the RPs. In the proposed WSF-based method, we incorporated rank vectors and probability distributions to acquire the WSF over the RPs.

1) OFFLINE PHASE

In the offline phase of the proposed method, the acquisition of RSS training data in the area of interest is performed. In other words, the RF signature data are collected at a few measurements points $S(S \subset \Lambda)$ to train the GP model, which predicts the RF signature at all locations without actual measurement. Note that the training data consist of the time averages of multiple RSS samples to reduce the effect of small-scale fading and avoid the potential overfitting problem of GPR [4]. The predicted RF signature map is fed to the APC-based RSS clustering module to extract RSS clustering information [16]. Moreover, the predicted signal strengths at each RP are arranged in descending order to create a rank

vector. Hence, the RF signature map of the proposed method is constructed as

$$RP_j = \{Id_j, (x_j, y_j), \Psi_j, R_j\}, \quad j \in 1, 2, \ldots, N, \tag{24}$$

where Id_j and (x_j, y_j) are the identification number and ground truth of j^{th} RP, respectively.

2) ONLINE PHASE

The fingerprinting positioning estimation result is performed in the online stage of the proposed WSF-based fingerprinting localization. It consists of two steps: a cluster matching and fine localization. First, observed online RSS data at an unknown location inside the testbed are smoothed. Here, we considered only $U'(U' < U)$ beacons for localization estimation to reduce the system's computational cost, which excludes the distantly deployed beacons in the localization estimation process. In this study, the size of U' was determined as the least number of beacons used at the training data measurement locations. U' beacons with larger RSS were preferably selected in the online phase. We propose the use of the exponential moving average (EMA) to minimize the RSS fluctuation:

$$\begin{aligned} \widehat{RSS}_t &= \beta \times RSS_t + (1-\beta) \times \widehat{RSS}_{t-1} \\ \beta &= \begin{cases} 0.7, & \text{tag at motion} \\ 0.5, & \text{tag at rest,} \end{cases} \end{aligned} \tag{25}$$

where $\beta (0 < \beta < 1)$ represents the smoothing factor. β close to one reduces the smoothing level, and β close to zero has a greater smoothing effect and is less responsive to recent RSS observation. $\widehat{RSS}_t$ and RSS_t are the estimated and observed RSS at an instant t. This study assumed β to be 0.7 when the tag was in motion (step is detected) due to frequent RSS changes and 0.5 during immobility giving equal preference to the previously smoothed result the latest RSS observation.

For a representative RP, given the estimated online RSS observation vector, $\hat{\Psi}_{r'}$, the following relation gives the posterior probability:

$$p(RP_j|\hat{\Psi}_{r'}) = \frac{p(\hat{\Psi}_{r'}|RP_j)p(RP_j)}{\sum_{i=1}^{N} p(\hat{\Psi}_{r'}|RP_i)p(RP_i)}, \tag{26}$$

where $p(\hat{\Psi}_{r'}|RP_j)$ is the likelihood described by the following relation:

$$p(\hat{\Psi}_{r'}|RP_j) = \prod_{u=1}^{U} \frac{1}{\sqrt{2\pi\sigma_u^2}} \exp\Big(-\frac{|\hat{\Psi}_{u,r'} - \mu_u|^2}{2\sigma_u^2}\Big). \tag{27}$$

Note that most of the existing studies on probability-based fingerprinting localization locate the user's position at the RP, which has the maximum likelihood [4], [26], [33]:

$$\hat{E}_{ML} = \underset{RP_j}{argmax}\, p(\hat{\Psi}_{r'}|RP_j). \tag{28}$$

Next, we estimated the SF distance of (7) at the RP_j by employing the stored and online rank vectors. Here, our proposed WSF was applied as a metric to find the k-nearest neighbor (k-NN) exploiting posterior probability, p_j (we used p_j to denote posterior probability for brevity):

$$WSF_j = \Big\{ \sum_{i=1}^{U'} |R_j(i) - R_{r'}(i)| \Big\} \times (1 - p_j). \tag{29}$$

- *Coarse localization*: Cluster matching is performed in coarse localization, as it helps to reduce both the positioning range and computational complexity and enhances the positioning accuracy. We define a set of cluster heads (namely, exemplars) and the members, RPs, grouped under a cluster head as C and N', respectively. The size of N' may vary with each cluster, where $N' < N$. To determine the exemplar RP, $WSF_e, e \in C$ for all cluster head RPs are calculated. The RP with the least WSF_e is selected as the exemplar RP.
- *Fine localization*: After the cluster head is determined, $WSF_{fine}, \forall fine \in \{1, 2, \ldots, N'\}$ for all the member RPs are calculated. The member RPs are sorted according to the ascending order of WSF_{fine}. The first k RPs are selected for fine localization. The fingerprinting localization estimation is performed by employing the posterior probabilities of the k RPs, and their known real location coordinate $(J_i[x_i, y_i])$ is determined as

$$\hat{L} = \frac{\sum_{i=1}^{k} p_i \times J_i}{\sum_{j=1}^{k} p_j}. \tag{30}$$

B. REAL-TIME FINGERPRINTING POSITION ERROR ESTIMATION

In the nearest neighbor (NN) approach for fingerprinting localization, the IPS returns only the RP position that offers the best match to the RF signature collected in the online phase. The k-NN can be exploited for better localization results where the IPS returns information about second, third, etc. best matches. As the RF signature map of adjacent RPs often exhibits highly overlapping signal strength properties, the positioning algorithm can estimate a tag to be at any nearby position (determined by k-NN or their weighted combination) to its actual position.

We exploited this observation and proposed a real-time position error estimation approach that first estimated the Euclidean error distance between $(J_i[x_i, y_i])$ and $\hat{L}$ as $D_i = \|J_i - \hat{L}\|$. Subsequently, the estimated error distances of the k-NN RPs were further combined with their respective posterior probabilities to compute $\hat{\epsilon}$ as

$$\hat{\epsilon} = \frac{\sum_{i=1}^{k} (D_i \times p_i)}{\sum_{j=1}^{k} p_j}. \tag{31}$$

C. PEDESTRIAN DEAD RECKONING

The PDR algorithm assumes a stepwise motion model (the user moves by making consecutive steps) to track the pedestrian described as [34]

$$\begin{aligned} x_t &= l_t + x_{t-1} \cos\theta_t \\ y_t &= l_t + y_{t-1} \sin\theta_t, \end{aligned} \tag{32}$$

where (x_t, y_t) is the estimated position at t^{th} step, which can be derived with known values of the step length (l_t) and heading direction θ_t. The PDR algorithm essentially requires three primary pieces of information to perform the user tracking operation:

- *Step detection*: Step detection helps in activity recognition (e.g., moving and standing still) by employing the accelerometer information. We adopted a peak detection approach for step detection as suggested in [11], which utilizes the vertical acceleration generated by the vertical strike when the user's foot hits the floor. Moreover, this approach utilizes two thresholds to filter out the false peaks caused by acceleration jitters that have very small magnitudes or short time intervals:

$$\begin{cases} \Delta T \geq T_{th} \\ |a_{mag} - g| \geq a_{th}, \end{cases} \tag{33}$$

  where ΔT, a_{mag}, and g represent the time interval between the adjacent peaks, the magnitude of acceleration (because vertical acceleration is affected by the tilting of the tag device), and the value of the local earth gravity, respectively. Similarly, T_{th} and a_{th} denote the time and acceleration magnitude thresholds, respectively. A true step is detected when (33) is valid.
- *Step length estimation*: Developing a generic model to estimate the step length for all users is a difficult task. Research has shown that step length for the same user mainly depends on his/her walking speed [11]. The empirical model [35] for step length estimation can be represented as follows:

$$l_t = H_t \times \sqrt[h]{a^t_{max} - a^t_{min}}, \tag{34}$$

  where a^t_{max} and a^t_{min} are the maximum and minimum vertical accelerations for step t.H_t and h represent the personalized coefficients for different users.
- *Orientation estimation*: The typical approach for orientation or heading direction estimation employs a magnetometer, which is sensitive towards electromagnetic devices and other metals in the localization environment. Moreover, orientation estimation employing a gyroscope is also prone to error due to the sensor noise accumulated during integration. We exploited a Kalman filter [3], [36] to estimate the user's heading direction while utilizing magnetometer and gyroscope readings.
  In [37], it is shown that the localization estimation error grows with an increase in the ground-truth reference path owing to a cumulative error in step detection and orientation estimation. In other words, the PDR approach yields good localization estimation for a short distance (PDR approach presented in [37] yields a 1 m localization error for the 20 m ground truth reference path). Therefore, in this study, the PDR localization of the proposed method was initialized with $\hat{L}$ at every $\mathcal{T}$ detected step.

D. AEKF FOR FUSING MULTISENSORY DATA

The widely accepted multisensory data fusion tool is the particle filter [38], [39]. However, the particle filter is ill-suited for real-time localization using a resource-limited smartphone owing to the substantial computation cost associated with its use. We employed a typical EKF for data integration as suggested in various studies [1], [11], [40], [41].

The general form of the discrete-time EKF system and the measurement models are

$$\begin{aligned} x_m &= \zeta_{m,m-1}(x_{m-1}) + s_{m-1} \\ z_m &= h_m(x_m) + o_m. \end{aligned} \tag{35}$$

Here,

x: State vector	**z**: Measurement vector
$\zeta()$: System model	$h()$: Measurement model
$m, m-1$: Data epochs	**s**: System noise
o: Measurement noise	

The system and measurement noises are further described as $s_{m-1} \sim N(0, Q_{m-1})$ and $o_m \sim N(0, R_m)$. Here, Q and R are the system and measurement noise covariance matrices, respectively.

As the EKF estimates the process state and then obtains feedback from the noisy measurements, it can be framed into two phases: the prediction and measurement correction phases (update). In our implementation, the PDR algorithm predicts the user's position at the next step during the prediction phase, which is corrected according to the position estimated from the proposed WSF-based fingerprinting localization during the measurement correction phase. The EKF estimates the current states and uncertainties in the prediction phase as

$$\begin{aligned} x^-_m &= W_{m,m-1}x^*_{m-1} \\ P^-_m &= W_{m,m-1}P^*_{m,m-1}W^T_{m,m-1} + Q_{m-1}, \end{aligned} \tag{36}$$

where **W** and **P** represent the state transition matrix and state error covariance matrix, respectively. In addition, the subscripts $^-$ and * denote the predicted and updated terms. The state transition matrix is defined as

$$W_{m,m-1} \approx \frac{\delta \zeta_{m,m-1}}{\delta x_{m,m-1}}. \tag{37}$$

Moreover, the observed measurement estimation is updated through the Kalman filter gain (K_m) as

$$\begin{aligned} K_m &= P^-_m H^T_m (H_m P^-_m H^T_m + R_m)^{-1} \\ x^*_m &= x^-_m + K_m(z_m - H_m x^-_m) \\ P^*_m &= (I - K_m H_m)P^-_m, \end{aligned} \tag{38}$$

where **I** is an identity matrix and **H** is a design matrix defined as $H \approx \frac{\delta h_m}{\delta x_m}$.

The elements in **R** can be set as empirical constants as discussed in [3]; the constants were determined using a fuzzy-logic system. However, such approaches have limited conditions that cannot fully represent real-time measurements. We suggest utilizing the real-time predicted errors given by (31) as the elements of **R** to realize the proposed AEKF.

The measurement noise covariance matrix of the proposed method is presented as follows:

$$R_m = diag([\hat{\epsilon}_m^2 \ \hat{\epsilon}_m^2]). \tag{39}$$

Moreover, assuming the system noise is linearly associated with the estimated step length and change in heading direction ($\Delta\theta_t$) [42], elements of $\mathbf{Q}$ can be defined as follows:

$$Q_m = diag([n_1 l_t \ n_2 \Delta\theta_t]). \tag{40}$$

where n_1 and n_2 are the linear coefficients.

VI. EXPERIMENTAL RESULTS AND DISCUSSION

A. EXPERIMENTAL SETUP

The proposed indoor localization solution was analyzed on two different testbeds with different signal attenuation environment. Testbed1 is the end-to-end hallway connecting different rooms, including an elevator, stairs, and lavatories, whereas Testbed2 consists of the main entrance of the building, a lobby, a study area, and some open space. Figure 6 presents pictures of both testbeds. Here, we employed Android smartphones for the evaluation. In particular, we used Samsung Galaxy S8 as a base device to acquire training data and used three more other Android phones, including Samsung Galaxy S10, LG G7, and Xiaomi MI Redmi 4 for the experiments. All the Android devices were equipped with a gyroscope, accelerometer, magnetometer, and a BLE receiver. Note that the tag devices were kept in the 'texting/messaging' position during the experiments. The default data delay (20K μs) was set for the gyroscope, magnetometer, and accelerometer. Similarly, the BLE beacons were deployed on the testbed (fifteen beacons on Testbed1 (115 m $\times$ 14 m) and seven beacons on Testbed2 (20 m $\times$ 35 m)), where advertisement interval and transmission power were set to 300 ms and +4 dBm, respectively.

In GPR-based fingerprinting localization, the training dataset's size is directly proportional to the localization accuracy [4]. However, as we intended to reduce the offline workload, the training dataset was expected to be smaller; therefore, the data collector visited a minimum number of measurement sites inside the localization interest area for optimum localization accuracy. Note that the regions near the training locations have smaller variances (that provides a confident interval for prediction) compared to other locations [16]. As there are no fixed rules to determine the training locations, we empirically chose each BLE beacon's vicinity as the training measurement place. Moreover, we solved the optimization problem of the GPR hyperparameter by employing the LM-BFGS algorithm [17], [18]. Note that LM-BFGS is an optimization algorithm in the family of quasi-newton methods, which approximates the BFGS [43] algorithm using a limited amount of system memory. Also, LM-BFGS is the widely used algorithm for parameter estimation in machine learning.

For RSS clustering, we adopted APC owing to its initialization-independent property and a better selection of exemplars. As the damping factor in the APC algorithm can be varied from 0.5 to 1 [5], [26], we chose the damping factor that corresponds to a minimum number of iterations for a lower computational cost. In particular, the damping factor and number of clusters for Testbed1 and Testbed2 were [0.65, 16] and [0.7, 10], respectively. Moreover, n_1 and n_2 in (40) were empirically set to 0.045 and 0.005, respectively.

(a)

(b)

FIGURE 6. Experiment environment: (a) Testbed1 and (b) Testbed2.

B. LOCALIZATION PERFORMANCE EVALUATION OF THE PROPOSED METHOD

To observe the consistency of localization performance in our test environment, we employed the cumulative distribution function (CDF) of the localization estimation error shown in Fig. 7. Here, ML refers to localization estimation by maximum likelihood, as given in (28), and Wk-NN is the weighted k-nearest neighbor fingerprinting. In Wk-NN, the RPs were sorted in ascending order of their SF distance to estimate the k-NN RPs where the value of k was selected as three for best localization results. Both the methods were integrated with PDR employing the EKF (i.e., ML+PDR and Wk-NN+PDR, respectively).

Furthermore, we used the average estimation error between the estimated location and the tag device's actual location to determine positioning methods' accuracy. In particular, we depicted the mean error as an indicator of localization accuracy with multiple tag devices at various locations inside

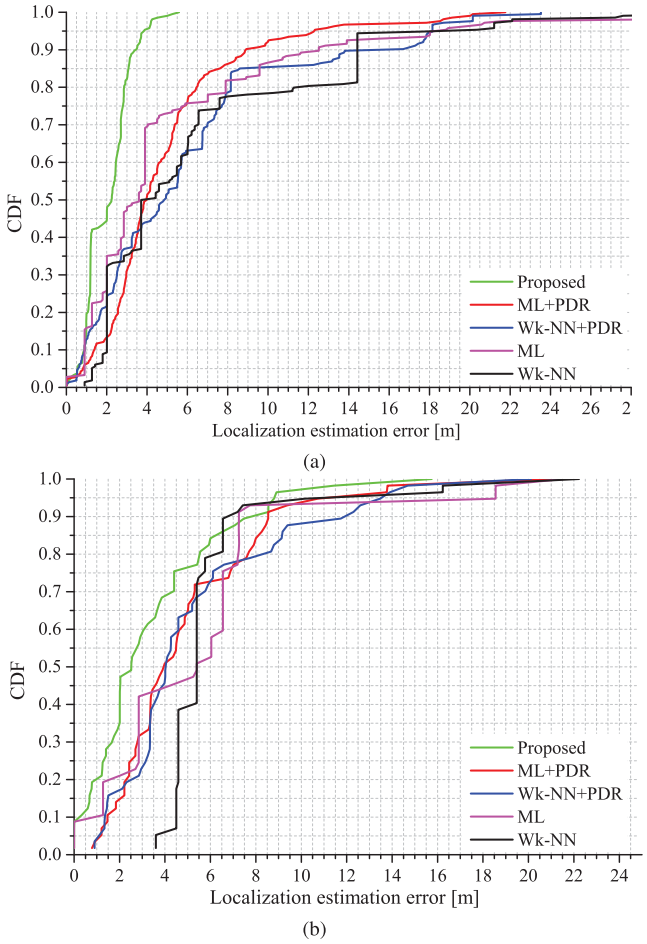

FIGURE 7. Cumulative probability of the localization estimation error: (a) Testbed1 and (b) Testbed2.

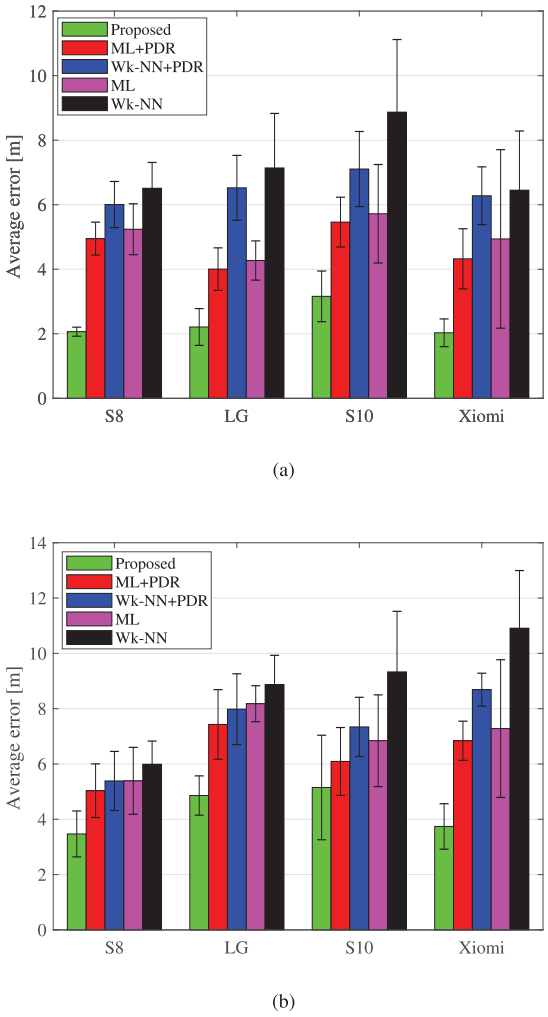

FIGURE 8. Average localization error observed in the different terminal devices: (a) Testbed1 and (b) Testbed2.

both the testbeds. The obtained result for both the testbeds is presented in Fig.8.

The CDF results in Fig. 7 and average localization results in Fig.8 show the superiority of the proposed approach against the methods under comparison. In particular, the mean error for the proposed method is [2.06m: Testbed1, 3.47m: Testbed2], while 95% of the error is under [3.8m: Testbed1, 8.8m: Testbed2]. On the other hand, the mean error and 95 percentile error for the existing methods are larger than the proposed method.

As shown in Fig. 8, the proposed approach yields acceptable localization results even with the least amount of training data points. Moreover, they reveal that the average positioning result can be controlled within 3 m in the open hallway (Testbed1) and below 5.5 m in the crowded wide region (Testbed2) by the proposed approach with heterogeneous terminal devices.

C. EFFECT OF DATA CLUSTERING ON COMPUTATIONAL COMPLEXITY

In conventional fingerprinting localization, the computational complexity increases with the size of the area of interest [44]. Considering a typical probabilistic fingerprinting method, its computational complexity in terms of $Big - O$ notation is $O(NU)$, where N is the total number of RPs (fingerprints to be compared), and U is the total number of access points deployed in the indoor environment. As stated earlier, the complexity grows with the size of N. Any clustering modules in IPS help to minimize the area of interest from N RPs to N' RPs during the coarse localization step, ($N' \ll N$). Therefore, the total number of fingerprints to be compared for fine localization is N', where the computational complexity becomes $O(N'U)$. Hence, clustering reduces the computational complexity by reducing the search space of RPs on the testbed.

For a detailed analysis, we calculated the consumed processing time for one epoch of positioning results for different localization methods. The observed relative positioning time for different positioning methods, where the proposed method's positioning time is t seconds, is illustrated in Fig. 9.

It is clear that clustering helps to reduce the computational cost of the positioning system.

TABLE 1. Comparison with various existing methods.

IPS	Complexity	Scalability	Robustness	Cost
Xin Li et. al [1]	High	Weak	Weak	Medium
S. Yiu et. al [4]	Moderate	Good	Weak	Low
You Li et. al [7]	High	Good	Weak	Low
Zhi-An Deng et. al [11]	Moderate	Weak	Weak	Low
Xin Li et. al [12]	Low	Weak	Weak	Low
S. Kumar et. al [19]	Moderate	Good	Weak	Low
You Li et. al [40]	High	Weak	Weak	Low
Ting guo et. al [45]	High	Weak	Weak	Low
Xianshan Li et. al [46]	High	Weak	Weak	Medium
Yi Cui et. al [47]	High	Weak	Weak	Low
Xiangyu Wang et. al [48]	High	Good	Weak	Low
Proposed	Low	Good	Good	Medium

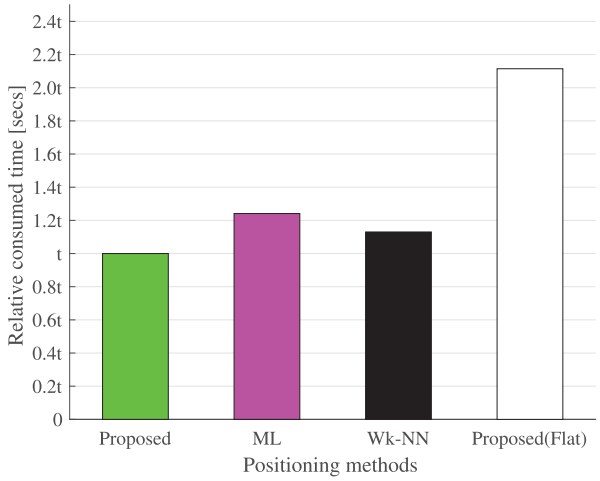

FIGURE 9. Performance comparison of positioning methods in terms of relative positioning time. (Proposed (Flat): proposed method without the coarse localization step).

D. TRAJECTORY ANALYSIS

The 2-D Cartesian coordinate estimated by our Android application during a user-walk in a predefined trajectory was recorded. The acquired localization estimation coordinate was mapped in the testbeds' graphical map, as shown in Fig. 10.

The red stars in Fig. 10 represent the deployed BLE beacons where the blue and black stars are the starting and ending points. The tracking result reveals that the proposed method can perform well in different radio environments.

E. COMPARISON WITH RELATED STATE-OF-ART APPROACHES

Other important performance metrics of an IPS are complexity, scalability, robustness, and cost in addition to the localization accuracy. Fingerprinting localization has relatively low scalability than lateral approaches (e.g., trilateration), where signal prediction and crowdsourcing help increase the method's scalability. Moreover, robust fingerprinting localization employs multiple RSS samples for positioning results. Hence, we compare our approach with some existing studies that are closely related to the proposed method. Note that the proposed method employs the signal prediction module and RSS filtration approach that enhance the scalability and robustness of the IPS system, respectively. A comparison of the different performance metrics is illustrated in Table 1.

F. COMPARISON OF RSS CLUSTERING AND DEVICE-BASED CLUSTERING

A separate RF signature map was created to compare the performance of RSS clustering and device-based clustering. Here, depending on the predicted RF signature data, all the testbed RPs were grouped under the beacons of their proximity. In other words, the RPs that shared a common BLE beacon were grouped in a cluster. The coarse localization phase in the device-based approach first identified the beacon with the strongest signal strength, and fine localization was performed in the searching space of RPs associated with the beacon. The cumulative probability of the localization estimation error induced by the proposed method at different data-clustering approaches is presented in Fig. 11.

As seen in Fig.11, the performance of the device-based clustering or the spatial filtering was comparable to the RSS clustering. We observed average localization errors of 1.92 m and 3.85 m in Testbed1 and Testbed2, respectively. Device-based clustering that does not require any fixed algorithm like APC and k-means clustering is easy to implement. However, if any hardware device (e.g., BLE beacon) malfunctions, the localization estimation error may significantly increase. Moreover, device-based clustering demands a dense deployment of beacons for better localization results.

G. DISCUSSIONS

In this paper, we focus on the practical limits and challenges of IPS that obstruct maintaining good performance metrics. In other words, in addition to the good localization accuracy, the suggested indoor localization approach is helpful towards maintaining low computational complexity, increase robustness and scalability, and mitigating the effect of heterogeneous terminal devices in a fingerprinting-based IPS. Moreover, the proposed method was implemented and evaluated in two different testbeds against different tag devices. For a better positioning result, the proposed method suggests

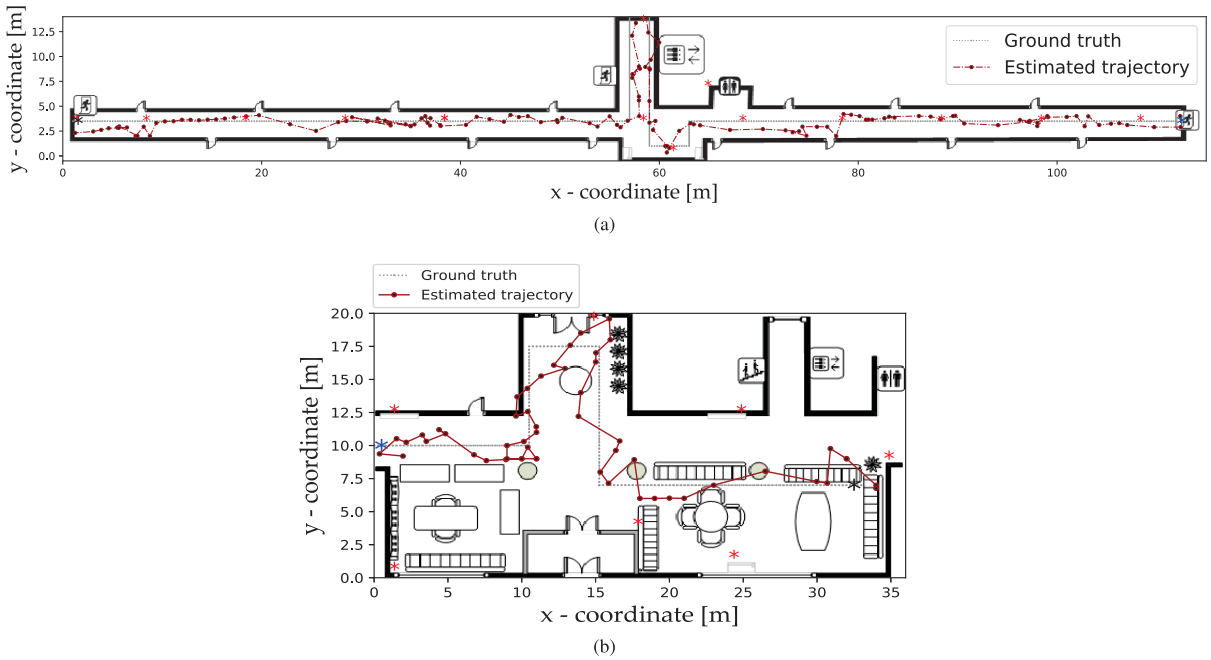

FIGURE 10. Smartphone user location estimated by the proposed method for (a) Testbed1 and (b) Testbed2.

using the signal source's rank and the RSS in the RF signature map during the offline phase and proposes WSF-based probabilistic fingerprinting for location estimation in the online phase. Furthermore, an FP error estimation approach is proposed to realize AEKF during multisensory data fusion.

The accuracy and precision of the proposed approach were measured using average localization error and CDF [13]. Fig. 7 illustrates the CDF of the localization estimation error at both the testbeds. Here, the superiority of the proposed method in Testbed2 is not as significant as in Testbed1 due to the testbeds' dimensions and BLE beacon deployment scenario. Testbed1 is an elongated hallway where beacons are deployed in a linear fashion, which helps generate a stable rank vector (as most beacons are far away at any measurement place in the testbed) to correct cluster selection in the online phase. However, the wrong cluster can be selected at some instances in Testbed2 owing to signal fluctuation. Moreover, the average localization error presented in Fig. 8 shows that the proposed method can yield a similarly significant result with heterogeneous tag devices. The accuracy and precision results and the tracking result (as shown in Fig. 10) imply that the proposed IPS can produce a reliable indoor localization solution.

Moreover, the localization system's scalability is its capability to perform well even during any change in the area of interest for localization and\or on the signal source. As with conventional fingerprinting, the requirement of offline workload makes it less scalable as compared to trilateration. The proposed method employs a supervised machine learning-based data prediction approach to infer the RSS at non-site-surveyed locations in the testbed. In other words, GPR was used for interpolating the RSS data that utilized significantly less training data (training data measurement

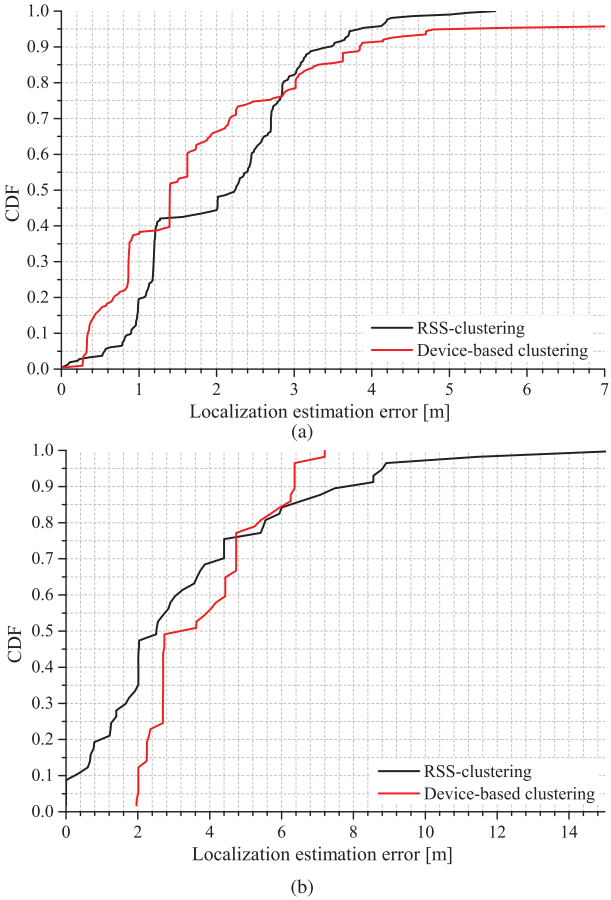

FIGURE 11. Cumulative probability of the localization estimation error: (a) Testbed1 and (b) Testbed2.

points were the vicinity of deployed beacons that consists of less than 5% of total test data (total RFs)). Hence, the offline

workload was reduced, resulting in increased scalability of the system.

Furthermore, the proposed IPS is computationally efficient both in terms of hardware and software. For example, the BLE beacon was used as a signal source supported by most present-day smartphones. Besides, RSS was used as a signal measurement principle, which is typically scanned by standard mobile phones for their routine functioning. The complexity depends on the computation load represented by the calculations required to perform positioning results regarding the software. The proposed IPS employs a clustering module to reduce the computation load. The proposed IPS' online phase employs EMA with a dynamic smoothing factor, enhancing the IPS' robustness.

VII. CONCLUSION

This paper proposes a smartphone-based indoor localization system that can suppress the existing challenges of conventional fingerprinting localization, improving the IPS. We introduce WSF-based probabilistic fingerprinting localization, which can overcome conventional fingerprinting in terms of localization accuracy and computational complexity. Considering the erroneous/incomplete RF signature map constructed by GPR prediction or crowdsourcing, the proposed fingerprinting localization can be an asset for maintaining the desired localization accuracy. Moreover, we propose a real-time fingerprinting position error estimation approach based on the proposed WSF to update the dynamic error of the AEKF. We implemented the suggested localization method using the RF signature map constructed by the machine-learning-based prediction approach. The data-clustering module balances the increased computational complexity of the proposed localization system. We realized GPR as a data prediction module and APC as an RSS data-clustering module. The proximity information of the deployed BLE beacons was used in device-based clustering, which worked as a spatial filter.

We employed BLE beacons as a low-cost solution because it has useful features in terms of power consumption and cost. The proposed localization solution was evaluated in two different testbeds, and the experimental results revealed an average error of 2.06 m in a hallway corridor and 3.47 m in a crowded and well-furnished indoor environment. Although meter-level localization accuracy is demanded, we note that the proposed localization solution's RF signature map consists of partial measurements, and the ground truth RSS for the remaining locations remain unknown. We show analytically and experimentally that data-clustering reduces the computational cost of a positioning system.

REFERENCES

[1] X. Li, J. Wang, and C. Liu, "A Bluetooth/PDR integration algorithm for an indoor positioning system," *Sensors*, vol. 15, no. 10, pp. 24862–24885, Sep. 2015.

[2] H. Zou, M. Jin, H. Jiang, L. Xie, and C. J. Spanos, "WinIPS: WiFi-based non-intrusive indoor positioning system with online radio map construction and adaptation," *IEEE Trans. Wireless Commun.*, vol. 16, no. 12, pp. 8118–8130, Dec. 2017.

[3] R. K. Yadav, B. Bhattarai, H.-S. Gang, and J.-Y. Pyun, "Trusted K nearest Bayesian estimation for indoor positioning system," *IEEE Access*, vol. 7, pp. 51484–51498, 2019.

[4] S. Yiu and K. Yang, "Gaussian process assisted fingerprinting localization," *IEEE Internet Things J.*, vol. 3, no. 5, pp. 683–690, Oct. 2016.

[5] S. Subedi, H.-S. Gang, and J.-Y. Pyun, "Regression assisted crowdsourcing approach for fingerprint radio map construction," in *Proc. Int. Conf. Indoor Positioning Indoor Navigat. (IPIN)*, Sep. 2019, pp. 1–7.

[6] B. Bhattarai, R. K. Yadav, H.-S. Gang, and J.-Y. Pyun, "Geomagnetic field based indoor landmark classification using deep learning," *IEEE Access*, vol. 7, pp. 33943–33956, 2019.

[7] Y. Li, Z. He, Z. Gao, Y. Zhuang, C. Shi, and N. El-Sheimy, "Toward robust crowdsourcing-based localization: A fingerprinting accuracy indicator enhanced wireless/magnetic/inertial integration approach," *IEEE Internet Things J.*, vol. 6, no. 2, pp. 3585–3600, Apr. 2019.

[8] H. Yang, W.-D. Zhong, C. Chen, A. Alphones, and P. Du, "QoS-driven optimized design-based integrated visible light communication and positioning for indoor IoT networks," *IEEE Internet Things J.*, vol. 7, no. 1, pp. 269–283, Jan. 2020.

[9] S. He and S.-H.-G. Chan, "Wi-Fi fingerprint-based indoor positioning: Recent advances and comparisons," *IEEE Commun. Surveys Tuts.*, vol. 18, no. 1, pp. 466–490, 1st Quart., 2016.

[10] H.-S. Gang and J.-Y. Pyun, "A smartphone indoor positioning system using hybrid localization technology," *Energies*, vol. 12, no. 19, p. 3702, Sep. 2019.

[11] Z.-A. Deng, Y. Hu, J. Yu, and Z. Na, "Extended Kalman filter for real time indoor localization by fusing WiFi and smartphone inertial sensors," *Micromachines*, vol. 6, no. 4, pp. 523–543, Apr. 2015.

[12] X. Li, J. Wang, C. Liu, L. Zhang, and Z. Li, "Integrated WiFi/PDR/smartphone using an adaptive system noise extended Kalman filter algorithm for indoor localization," *ISPRS Int. J. Geo-Inf.*, vol. 5, no. 2, p. 8, 2016.

[13] S. Subedi and J.-Y. Pyun, "A survey of smartphone-based indoor positioning system using RF-based wireless technologies," *Sensors*, vol. 20, no. 24, p. 7230, Dec. 2020.

[14] P. Richter and M. Toledano-Ayala, "Revisiting Gaussian process regression modeling for localization in wireless sensor networks," *Sensors*, vol. 15, no. 9, pp. 22587–22615, Sep. 2015.

[15] K. Liu, Z. Meng, and C.-M. Own, "Gaussian process regression plus method for localization reliability improvement," *Sensors*, vol. 16, no. 8, p. 1193, Jul. 2016.

[16] S. Subedi and J.-Y. Pyun, "Lightweight workload fingerprinting localization using affinity propagation clustering and Gaussian process regression," *Sensors*, vol. 18, no. 12, p. 4267, Dec. 2018.

[17] R. H. Byrd, P. Lu, J. Nocedal, and C. Zhu, "A limited memory algorithm for bound constrained optimization," *SIAM J. Scientific Comput.*, vol. 16, no. 5, pp. 1190–1208, Sep. 1995.

[18] C. Zhu, R. H. Byrd, P. Lu, and J. Nocedal, "L-BFGS-B: FORTRAN subroutines for large scale bound constrained optimization," EECS Dept., Northwestern Univ., Tech. Rep. NAM-11, 1994.

[19] S. Kumar, R. M. Hegde, and N. Trigoni, "Gaussian process regression for fingerprinting based localization," *Ad Hoc Netw.*, vol. 51, pp. 1–10, Nov. 2016.

[20] M. Youssef and A. Agrawala, "The horus WLAN location determination system," in *Proc. 3rd Int. Conf. Mobile Syst., Appl., Services (MobiSys)*, 2005, pp. 205–218.

[21] N. Hernández, M. Ocaña, J. Alonso, and E. Kim, "Continuous space estimation: Increasing WiFi-based indoor localization resolution without increasing the site-survey effort," *Sensors*, vol. 17, no. 12, p. 147, Jan. 2017.

[22] L. Kanaris, A. Kokkinis, A. Liotta, and S. Stavrou, "Fusing Bluetooth beacon data with Wi-Fi radiomaps for improved indoor localization," *Sensors*, vol. 17, no. 4, p. 812, Apr. 2017.

[23] E. Gokcay and J. C. Principe, "Information theoretic clustering," *IEEE Trans. Pattern Anal. Mach. Intell.*, vol. 24, no. 2, pp. 158–171, Feb. 2002.

[24] D. Dueck, *Affinity Propagation: Clustering Data by Passing Messages*. London, U.K.: Citeseer, 2009.

[25] J. C. Bezdek, R. Ehrlich, and W. Full, "FCM: The fuzzy C-means clustering algorithm," *Comput. Geosci.*, vol. 10, nos. 2–3, pp. 191–203, Jan. 1984.

[26] Z. Tian, X. Tang, M. Zhou, and Z. Tan, "Fingerprint indoor positioning algorithm based on affinity propagation clustering," *EURASIP J. Wireless Commun. Netw.*, vol. 2013, no. 1, p. 272, Dec. 2013.

[27] S. Subedi, H.-S. Gang, N. Y. Ko, S.-S. Hwang, and J.-Y. Pyun, "Improving indoor fingerprinting positioning with affinity propagation clustering and weighted centroid fingerprint," *IEEE Access*, vol. 7, pp. 31738–31750, 2019.
[28] P. Diaconis and R. L. Graham, "Spearman's footrule as a measure of disarray," *J. Roy. Stat. Soc., B (Methodol.)*, vol. 39, no. 2, pp. 262–268, Jan. 1977.
[29] R. Kumar and S. Vassilvitskii, "Generalized distances between rankings," in *Proc. 19th Int. Conf. World Wide Web (WWW)*, 2010, pp. 571–580.
[30] C. Rasmussen and C. Williams, *Gaussian Processes for Machine Learning*. Cambridge, MA, USA: MIT Press, 2006.
[31] J. Bergstra and Y. Bengio, "Random search for hyper-parameter optimization," *J. Mach. Learn. Res.*, vol. 13, pp. 281–305, Feb. 2012.
[32] J. Snoek, H. Larochelle, and R. P. Adams, "Practical Bayesian optimization of machine learning algorithms," in *Proc. Adv. Neural Inf. Process. Syst.*, 2012, pp. 2951–2959.
[33] J. Luo and L. Fu, "A smartphone indoor localization algorithm based on WLAN location fingerprinting with feature extraction and clustering," *Sensors*, vol. 17, no. 6, p. 1339, Jun. 2017.
[34] H. Ju, S. Y. Park, and C. G. Park, "A smartphone-based pedestrian dead reckoning system with multiple virtual tracking for indoor navigation," *IEEE Sensors J.*, vol. 18, no. 16, pp. 6756–6764, Aug. 2018.
[35] R. Zhang, A. Bannoura, F. Hoflinger, L. M. Reindl, and C. Schindelhauer, "Indoor localization using a smart phone," in *Proc. IEEE Sensors Appl. Symp.*, Feb. 2013, pp. 38–42.
[36] Z. Chen, Q. Zhu, and Y. C. Soh, "Smartphone inertial sensor-based indoor localization and tracking with iBeacon corrections," *IEEE Trans. Ind. Informat.*, vol. 12, no. 4, pp. 1540–1549, Aug. 2016.
[37] W. Kang and Y. Han, "SmartPDR: Smartphone-based pedestrian dead reckoning for indoor localization," *IEEE Sensors J.*, vol. 15, no. 5, pp. 2906–2916, May 2015.
[38] F. Evennou and F. Marx, "Advanced integration of WiFi and inertial navigation systems for indoor mobile positioning," *EURASIP J. Adv. Signal Process.*, vol. 2006, no. 1, p. 164, Dec. 2006.
[39] S. Xu, R. Chen, Y. Yu, G. Guo, and L. Huang, "Locating smartphones indoors using built-in sensors and Wi-Fi ranging with an enhanced particle filter," *IEEE Access*, vol. 7, pp. 95140–95153, 2019.
[40] Y. Li, Z. Gao, Z. He, Y. Zhuang, A. Radi, R. Chen, and N. El-Sheimy, "Wireless fingerprinting uncertainty prediction based on machine learning," *Sensors*, vol. 19, no. 2, p. 324, Jan. 2019.
[41] S. Qiu, Z. Wang, H. Zhao, K. Qin, Z. Li, and H. Hu, "Inertial/magnetic sensors based pedestrian dead reckoning by means of multi-sensor fusion," *Inf. Fusion*, vol. 39, pp. 108–119, Jan. 2018.
[42] B. Feng, W. Tang, G. Guo, and X. Jia, "An improved pedestrian ttracking method based on Wi-Fi fingerprinting and pedestrian dead reckoning," *Sensors*, vol. 20, no. 3, p. 853, Feb. 2020.
[43] Y.-H. Dai, "A perfect example for the BFGS method," *Math. Program.*, vol. 138, nos. 1–2, pp. 501–530, Apr. 2013.
[44] A. Khalajmehrabadi, N. Gatsis, and D. Akopian, "Modern WLAN fingerprinting indoor positioning methods and deployment challenges," *IEEE Commun. Surveys Tuts.*, vol. 19, no. 3, pp. 1974–2002, 3rd Quart., 2017.
[45] T. Guo, C. Li, C. Liu, and H. Huang, "A fusion indoor positioning algorithm based on the improved WKNN and pedestrian dead reckoning," in *Proc. IEEE 20th Int. Conf. Commun. Technol. (ICCT)*, Oct. 2020, pp. 552–558.
[46] X. Li, Y. Shao, and F. Zhao, "An indoor positioning approach using smartphone based on PDR and EKF," in *Proc. 15th IEEE Conf. Ind. Electron. Appl. (ICIEA)*, Nov. 2020, pp. 182–187.
[47] Y. Cui, Y. Zhang, Y. Huang, Z. Wang, and H. Fu, "Novel WiFi/MEMS integrated indoor navigation system based on two-stage EKF," *Micromachines*, vol. 10, no. 3, p. 198, Mar. 2019.
[48] X. Wang, X. Wang, S. Mao, J. Zhang, S. C. G. Periaswamy, and J. Patton, "Indoor radio map construction and localization with deep Gaussian processes," *IEEE Internet Things J.*, vol. 7, no. 11, pp. 11238–11249, Nov. 2020.

SANTOSH SUBEDI received the B.E. degree in electronics and communication engineering from Tribhuvan University, Nepal, in 2010, the M.Tech. degree in communication engineering from the National Institute of Technology Karnataka, India, in 2014, and the Ph.D. degree from Chosun University, South Korea, in 2019. From 2019 to 2020, he worked as a Postdoctoral Researcher with the IT Research Institute, Chosun University. In 2020, he joined the Department of Information and Communication Engineering, Chosun University, as an Assistant Professor. His research interests include indoor positioning techniques, wireless sensor networks, wireless communication systems, IoT based services, and machine learning/deep learning.

DAE-HO KIM received the B.S. and M.S. degrees in information and communication engineering from Chosun University, South Korea, in 2015 and 2017, respectively, where he is currently pursuing the Ph.D. degree. His research interests include embedded systems, wireless sensor networks, IoT based communications, and indoor positioning techniques.

BEOM-HUN KIM received the B.S. degree in computer engineering and the M.S. degree in software convergence engineering from Chosun University, South Korea, in 2010 and 2015, respectively, where he is currently pursuing the Ph.D. degree in information and communication engineering. His research interests include signal processing, indoor positioning systems, machine learning, and deep learning. He is also a member of the "Wireless and Mobile Communication System Laboratory."

JAE-YOUNG PYUN received the B.S. degree from Chosun University, the M.S. degree from Chonnam University, and the Ph.D. degree from Korea University, South Korea, all in electronics engineering, in 1997, 1999, and 2003, respectively. From 2003 to 2004, he was with Samsung Electronics Company Ltd., where he was involved in the research and development of mobile phone communication systems. In 2004, he joined the Department of Information and Communication Engineering, Chosun University, where he is currently a Professor. His research interests include network protocols over WSN, indoor positioning, and video communication. He has been a member of IEICE, IEEK, and KICS, since 2004.